J Mater Sci (2009) 44:5861–5871
DOI 10.1007/s10853-009-3827-7

Effect of nanoclays on physico-mechanical properties and adhesion of polyester-based polyurethane nanocomposites: structure–property correlations

Pradip K. Maji · Prasanta K. Guchhait · Anil K. Bhowmick

Received: 30 May 2009 / Accepted: 20 August 2009 / Published online: 2 September 2009

Abstract Polyester–polyurethane nanocomposites based on unmodified and modified montmorillonite clays were compared in terms of their morphology, mechanical, thermal, and adhesive properties. Excellent dispersion of the modified nanoclay in polymer with 3 wt% loading was confirmed from X-ray diffraction, and low-, and high-magnification transmission electron micrographs. The properties of the clay-reinforced polyurethane nanocomposites were a function of nature and the content of clay in the matrix. The nanocomposite containing 3 wt% modified clay exhibits excellent improvement in tensile strength (by ~100%), thermal stability (20 °C higher), storage modulus at 25 °C (by ~135%), and adhesive properties (by ~300%) over the pristine polyurethane.

Introduction

Hybrid organic–inorganic nanocomposites based on layered silicates have received special attention recently due to very low cost of the inorganic counterpart as well as its very high reinforcement ability, relatively simple preparation, and fairly predictable reinforcement property when incorporated into a polymer [1–4]. The thermomechanical responses of polymers, which provide limitations of their practical use, are favorably altered by the addition of a trace amount of nanofillers. The way to optimal nanocomposites formation requires maximizing the four following structural parameters: (1) the particle aspect ratio, (2) particle dispersion, (3) particle packing (or alignment), and (4) polymer to particle interfacial stress transfer [5–9]. Among the nanofillers, montmorillonite clay is one of the important classes of nanofillers. Ammonium surfactants are usually used to modify montmorillonite clay in order to gain better interaction between the hydrophilic aluminosilicate and the organophilic polymer matrix and to achieve the best exfoliation structure. Previous studies in our laboratory have shown that styrene butadiene rubber-based nanocomposites have the best exfoliation when the organoclay is formed from a surfactant with long alkyl tail [10].

Because of the enhancement and novel properties of polymer/layered silicate nanocomposites over pure polymer, many new nanocomposites based on polymer/clay have been investigated, such as epoxy resin/clay [11], styrene (ethylene-*co*-butylene)styrene/clay [12], styrene butadiene/clay [10], fluoroelastomer/clay [13] nanocomposites, and so on.

Polyurethane copolymers are important subclass of the family of thermoplastic elastomers. They are composed of short, alternating polydisperse blocks of soft and hard segments [14]. It is one of the most useful commercial polymer materials. In previous preparation route to clay/polyurethane nanocomposites, the approach was to physically mix nanoclay with polyurethane [15–17]. The intercalated silicates resulted from physical trap forces such as polar, hydrogen bonding, or shear between the clay and the polymer.

In this article, we first prepare polyester polyurethane prepolymer/nanoclay hybrid in the tetrahydrofuran (THF) solution by use of predispersed nanoclay. Then, the hybrid

P. K. Maji · P. K. Guchhait · A. K. Bhowmick (✉)
Rubber Technology Centre, Indian Institute of Technology, Kharagpur 721302, India
e-mail: anilkb@rtc.iitkgp.ernet.in; director@iitp.ac.in

Present Address:
A. K. Bhowmick
Indian Institute of Technology, Patna 800013, India

resins were cured by isocyanates to obtain polyester-based polyurethane/nanoclay hybrid film. Modified and unmodified nanoclays were chosen for investigating the effect of the nature and loading of clay on the properties of the nanocomposites. Obviously, the clay in the polyurethane matrix influences the microstructure and performance of polyurethanes. An understanding of the extent of improvement and the reasons are important, since polyester-based polyurethanes have been widely used in automobiles, space, defense, adhesives, coatings, and so on. This is part of our ongoing studies on structure–property relationship of various special purpose elastomeric nanocomposites [10, 12, 13, 18–20].

Experimental

Materials

The isocyanate crosslinkable polyester polyurethane prepolymer (Urepan 600) was supplied by M/s Rhein Chemie Rhenau GmbH, Germany. According to the supplier's instructions, in the production of this material, a polyester was firstly prepared by reacting diethylene glycol and adipic acid. This was then reacted with toluene di-isocyanate in such a way, so that the chain ends were hydroxyl. The hydroxyl value that was determined by the Karl Fischer Titration method was 25.8 mg KOH/g. Toluene-2, 4-diisocyanate (TDI) was purchased from Merck Schuchardt OHG, Hohenbrunn, Germany. Cloisite 30B (modified clay) containing 90 mequiv of quaternary ammonium ions/100 g of clay and Cloisite Na^+ (unmodified clay) were purchased from Southern Clay Products, Gonzales, TX, USA. The quaternary ammonium ion has a structure of $N^+(CH_2CH_2OH)_2(CH_3)T$, with T representing an alkyl group of approximately 65% C_{18}, 30% C_{16}, and 5% C_{14} for Cloisite 30B. Dry solvent, THF, was purchased from Rankem, Kolkata, India.

Nanocomposite preparation

Polyester–polyurethane prepolymer rubber was lightly masticated in an open two roll mill for two to three passes at ambient condition. 10 g of masticated rubber was soaked in a 90 g of THF overnight, stirred with high-speed mixer for 1 h at room temperature. The homogeneous solution was thus obtained. A dispersion of nanoclay was made in THF and the mixture was cooled at 0–10 °C and passed through ultrasonicator for half an hour. THF dispersion containing nanoclay was added to polyurethane prepolymer solution with vigorous stirring. The equivalent amount of curing agent (TDI) to that of PU prepolymer was calculated from hydroxyl value of PU prepolymer and was found to be 0.40 g. The excess amount of TDI (total of 2 g or 0.0011 moles) that was used to form the 3D network of the PU prepolymer was selected from the general formulation of polyurethane elastomers [21, 22]. The addition of excess TDI enables reaction to occur at the urethane groups with the formation of allophanate branch points (shown in Fig. 1) without imparting any significant side reactions. The crosslinking reaction scheme is given in Fig. 1. The solution was cast onto circular quartz plates after addition and homogeneous mixing of the curing agent. The solvent was allowed to dry under natural air convection under cover for overnight at room temperature. To investigate the effect of clay on the mechanical, adhesive, and thermal properties and the microstructure of the PU/clay nanocomposite, three concentrations (1, 3, and 5 wt%) of the modified clay and one concentration (3 wt%) of the unmodified clay were used.

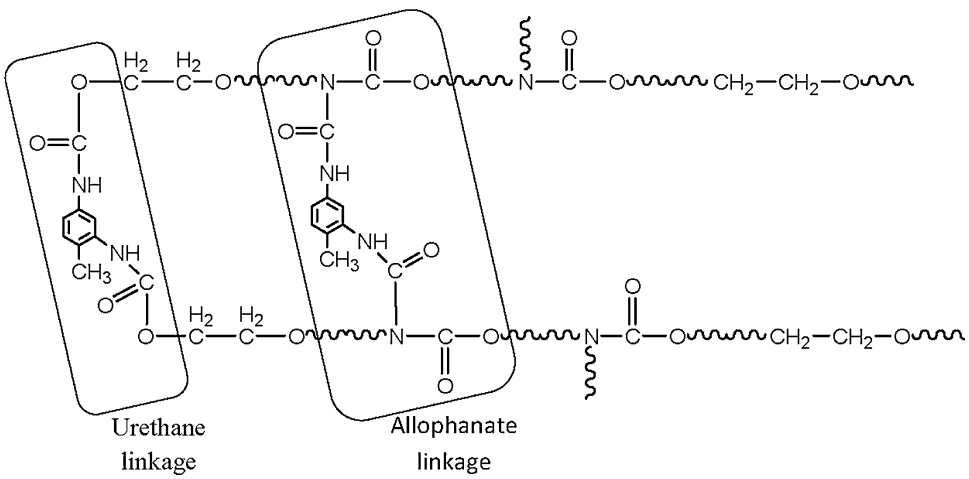

Fig. 1 Reaction scheme of crosslinking of polyester polyurethane prepolymer with TDI

Characterization

FTIR spectroscopic studies

FTIR studies were carried out in dispersive mode on thin film samples ($\sim$100 μm) using a Perkin-Elmer FTIR spectrophotometer (model spectrum RX I), within a range of 400–4400 cm^{-1} using a resolution of 4 cm^{-1}. An average of 16 scans was reported for each sample.

X-ray diffraction studies

The X-ray diffraction (XRD) patterns of the samples were recorded in a Philips X-ray diffractometer (model PW-1710) at crystal monochromated Cu Kα radiation in the angular range 2–10° (2θ) at 40 kV operating voltage and 20 mA current.

Transmission electron microscopy

The samples for transmission electron microscopy (TEM) analysis were prepared by ultracryomicrotomy with a Leica Ultracut UCT (Leica Mikrosystems GmbH, Vienna, Austria). Freshly sharpened glass knives with cutting edges of 45° were used to obtain cryosections of 50–70 nm thickness. Because these samples were elastomeric in nature, the sample and glass knife temperatures during ultracryomicrotomy were kept constant at −50 and −60 °C, respectively [these temperatures were well below the glass transition temperatures (T_g's) of PUs]. The cryosections were collected individually in a sucrose solution and directly supported on a copper grid of 300 meshes in size. Microscopy was performed with a JEOL JEM 2010 TEM instrument (Japan), operating at an accelerating voltage of 120 kV.

Dynamic mechanical thermal analysis

The dynamic mechanical thermal analysis (DMTA) spectra of the samples were obtained by using DMTA of TA Instruments (model 2980 V1.7B). The sample specimens were analyzed in tensile mode at a constant frequency of 1 Hz, a strain of 0.01%, and a heating rate of 2 °C/min. The data were analyzed by TA Universal analysis software on a TA computer attached to the machine. The storage modulus (E') and loss tangent (tan δ) were measured as a function of the temperature for all of the samples under identical conditions. The temperature corresponding to the peak in the tan δ versus temperature plot was taken as the glass–rubber transition temperature (T_g).

Thermogravimetric analysis

Thermogravimetric analysis (TGA) was carried out in TA Instruments (model Q50), at a heating rate of 10 °C/min under a nitrogen atmosphere up to 600 °C. The data were analyzed by TA Universal analysis software on a TA computer attached to the machine. A small amount of material (around 5 mg) was used for the TGA study. In the thermal testing experiment, there is ±1 °C variation in the temperature and ±0.1 g variation in the reproducibility of mass. The reported values are the average of at least three tests performed.

Tensile properties

Tensile specimens were punched out from the cast sheets using ASTM Die-C. The tests were carried out as per the ASTM D 412-98 method in a Universal Testing Machine (Zwick 1445) at a crosshead speed of 500 mm/min at 25 °C. The average of three tests is reported here.

Lap shear strength

The lap shear strength between aluminum and aluminum was measured as per the ASTM D 1002-05 method in a Universal Testing Machine (Hounsfield H10KS) at a crosshead speed of 1.3 mm/min. The average of three tests is reported here.

Results and discussion

FTIR spectroscopic studies

The FTIR spectra of the unmodified clay (NA) and the modified clay (CB) are shown in Fig. 2. As it can be seen in Fig. 2a, the characteristic peaks of unmodified clay at 3632 cm^{-1} (–OH stretching), 1047 cm^{-1} (Si–O in plane stretching), 798 cm^{-1} (Si–O stretching), 623 cm^{-1} (Al–O and Si–O out of plane vibration), 522 cm^{-1} (Al–O–Si deformation) as well as a weak broad absorption at 3440 cm^{-1} (H–OH hydrogen bonded water), and 1640 cm^{-1} (–OH deformation of entrapped water) are observed. These peaks are also noted in the modified clay. As shown in Fig. 2b, the absorbances at 1300, 500, and 3632 cm^{-1} are almost identical to those of the unmodified clay, indicating that the main structure of the silicate layer is unchanged. On the other hand, the absorbances in the region of 2925–2852 cm^{-1} of $–CH_2–$ and $–CH_3$ stretching frequencies and 3375 cm^{-1} of ionic bonded N–H stretching vibration of tertiary amine indicate that the interlayer water is replaced by the modifier by a cation exchange process.

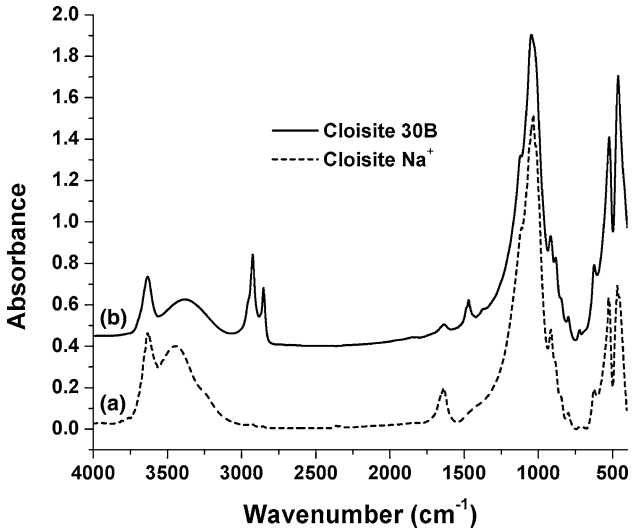

Fig. 2 FTIR spectra of (*a*) unmodified clay and (*b*) modified clay

To understand the possible reactions that may occur among the reactants (TDI, polyester polyurethane prepolymer, and modified clay), the FTIR spectra of polyester polyurethane prepolymer, TDI cured PU prepolymer (PUP), and PU nanocomposites containing 5 wt% modified clay ($PUCB_5$) are recorded in Fig. 3. As seen in Fig. 3a, the characteristic absorptions peaks of the Urepan 600 are observed at 3306 cm^{-1} (N–H stretching frequency), 2925–2852 cm^{-1} (–CH_2– and –CH_3 stretching frequencies), 1731 cm^{-1} (carbonyl urethane stretching), 1526 cm^{-1} (CHN vibration), 1223 cm^{-1} (coupled C–N and C–O stretching), and 1079 cm^{-1} (C–O stretching). Comparison of Fig. 3a with Fig. 3b indicates that all the characteristic absorptions of Urepan 600 remain unchanged in the cured PU (PUP). But the urethane characteristic peaks at 1732 and 1526 cm^{-1} are enhanced due to the formation of more number of urethane linkages during the course of the curing reaction. Absence of peak at 2270 cm^{-1} (–NCO group) confirms that all the TDI have been used in the curing reaction. Besides, the characteristic absorption peaks of benzene ring of TDI are observed in the region of 900–675 cm^{-1} (C–H deformation). When Fig. 3c is compared with Fig. 3b, it is evident that the characteristic absorption peaks at 522 cm^{-1} (Al–O–Si deformation) and 1047 cm^{-1} (Si–O in plane stretching) are observed in the cured PU nanocomposites ($PUCB_5$). Furthermore, the extra absorptions at 3700–3400 cm^{-1} (N–H stretching) and 1240 cm^{-1} (amide vibration) indicate the formation amide structure between the modified clay and the PU matrix.

The possibility of reaction between clay and polymer chains has also been investigated by monitoring the FTIR spectrum. For this purpose, we have resorted to Soxhlet extraction of the composite materials to determine the amounts of residue. It is interesting to note that a trace amount of polyurethane chains is associated with the residue of $PUCB_3$. This clearly suggests that the –CH_2CH_2OH groups in the surfactant of Cloisite 30B participate in the reaction. The residues were characterized by FTIR to determine their chemical nature. It is seen from the FTIR spectra in Fig. 4a that the residue with Cloisite 30B has the characteristic peaks at 1731 cm^{-1} (carbonyl urethane stretching), 1526 cm^{-1} (C–NH– vibration), 1223 cm^{-1} (coupled C–N and C–O stretching), 1079 cm^{-1} (C–O stretching), 522 cm^{-1} (Al–O–Si deformation), and 1047 cm^{-1} (Si–O in plane stretching), indicating the presence of

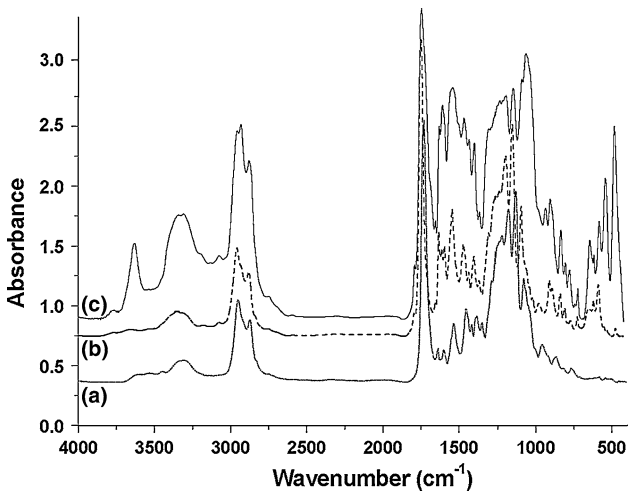

Fig. 3 FTIR spectra of (*a*) polyester polyurethane prepolymer; (*b*) isocyanate cured polyester polyurethane (PUP); and (*c*) isocyanate cured polyester polyurethane containing 5 wt% modified clay ($PUCB_5$)

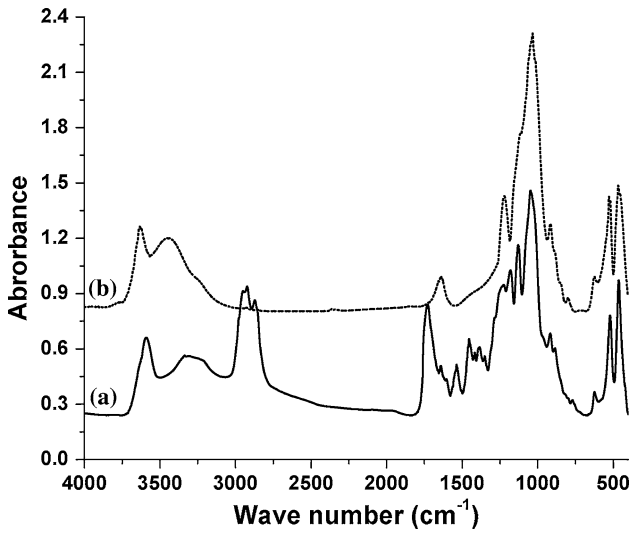

Fig. 4 FTIR spectra of Soxhlet extracted residues of composites with 3 wt% clay (*a*) $PUCB_3$ and (*b*) $PUNA_3$

polyurethane chains and the clay particles in the residue. Figure 4b for non-reactive clays (Cloisite Na^+), however, shows only the prominent Si–O stretching of the clay, indicating non-compatibility with the polyurethane chains. Some polymer chain ends with –NCO groups come closer to the vicinity of the clay galleries during nanocomposites preparation and react with $–CH_2CH_2OH$ group of the quaternary ammonium ions to produce urethane linkage, –CO–NH–, leading to a fine dispersion of the clay particles, as seen in the TEM image discussed later.

XRD studies

The X-ray diffractograms of the unmodified and the modified clays and their nanocomposites are shown in Fig. 5. The intergallery spacings of different clays and nanocomposite are reported in Table 1. The peak 2θ value at 7.5° corresponding to *d*-spacing of 1.17 nm appears in the case of the unmodified nanoclay, whereas in the amine-modified organophilic clays, the intergallery spacing increases to 1.84 nm, due to the impregnation of the amines and the hydrogenated tallow group into the gallery stacks. The bulkier and branched amines have larger intergallery spacing. The clay, intercalated and organophilic, permits adequate space for polymer chains to enter into the clay galleries. The results of the unmodified and the modified clays are in good agreement with those reported earlier from our laboratory [10, 18]. The unmodified clay galleries in the $PUNA_3$ composites are expanded slightly by the PU chains, as evident from the peak at 5.9°. This peak corresponds to a gallery gap of 1.49 nm, which is larger than that of the unmodified clay (1.17 nm). Intercalation may be inferred in the aforesaid system, as there is a 27% increase in gallery spacing. Here, the polymer–clay interaction is expected to be much lower, as the clay is hydrophilic in nature and the polymer is an organic one. A similar observation is made with SBR [10]. On the other hand, there is no peak in the XRD of $PUCB_1$ and $PUCB_3$. This indicates disordering and good dispersion of the clay in the polymer matrix. The plausible reason for better dispersion of the clay layers is a better interaction between the modified (hydrophobic in nature) nanoclay and the organic polymer matrix as indicated by FTIR spectroscopy (Fig. 4a) and also increased gallery height. Moreover, the effect of steric factors caused by the bulky amines and lower concentration of clay cannot be ruled out. However, intercalation is observed in the case of $PUCB_5$. There is a small hump at 4.3°, corresponding to the *d*-spacing of 2.06 nm. This may be due to the filler agglomeration at higher filler loading. The results indicate that there is a tendency toward agglomeration of the modified clay particles at higher loadings. This inference has been further strengthened by the morphological studies in the subsequent section. There are examples of clay exfoliation in many polymers like nylon-6 [23], polypropylene [24], and so on.

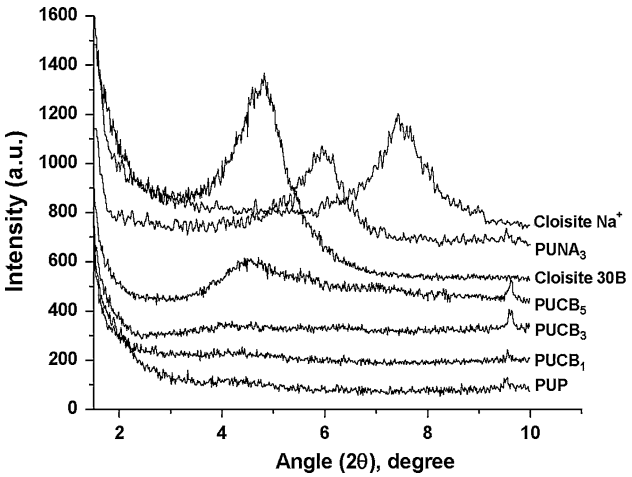

Fig. 5 XRD patterns of different clays and their nanocomposites having different loadings

Table 1 Gallery spacing of different clays and nanocomposites

Sample No.	2θ (degree)	Gallery gap (nm)
Cloisite Na^+	7.5	1.17
Cloisite 30B	4.8	1.84
$PUNA_3$	5.9	1.49
$PUCB_1$	No peak	–
$PUCB_3$	No peak	–
$PUCB_5$	4.3	2.06

Transmission electron microscopy

The most direct measure of the dispersion of these nanometer-scale silicates in polyurethane can typically be found in the TEM micrographs of the cross section of polymer nanocomposites as demonstrated in most of the literature [8]. In Fig. 6a, in the case of high-magnification image of $PUCB_1$ containing 1 wt% modified clay, intercalated domains having a collection of four to five nearly parallel-layered silicates with spacing from 10 to 100 nm are observed and most of the clays are exfoliated. The thickness of the layered silicate (dark lines) is about 1.0 nm. For the case of high-magnification TEM image of $PUCB_3$ containing 3 wt% modified clay, the space between the layered silicates is decreased to ~8–50 nm, and the silicates layers are mostly delaminated or exfoliated in nature, as shown in Fig. 6b. In Fig. 6c, for $PUCB_5$ containing 5 wt% modified clay, the space between layered silicates is further decreased to about 4–10 nm, and a larger portion of silicates becomes intercalated or agglomerated as compared to

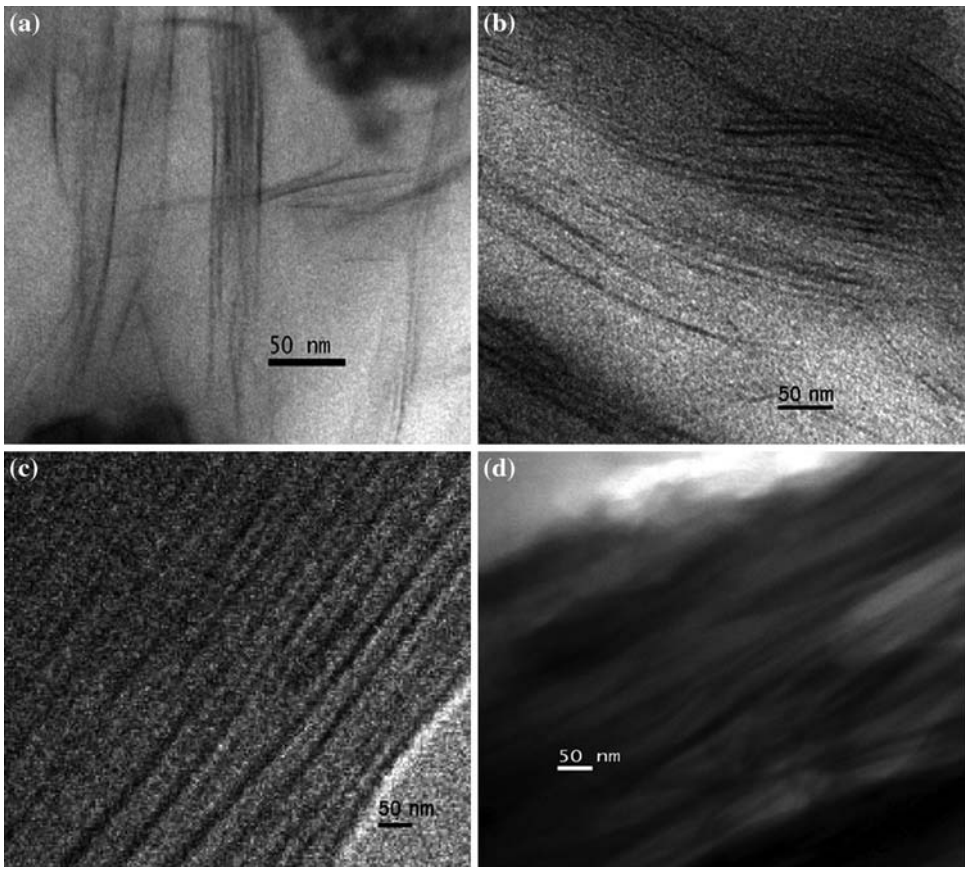

Fig. 6 High-magnification TEM micrographs of different PUs at various clay loadings: **a** $PUCB_1$; **b** $PUCB_3$; **c** $PUCB_5$; **d** $PUNA_3$

$PUCB_3$ containing 3 wt% modified clay. The dispersion of the silicates in polyurethane can actually adopt a bi-model structure, which consists of both intercalated and exfoliated states. To see the global dispersion of the clay in the polyurethane matrix, low-magnification TEM photograph has been taken. The micrographs show a homogeneous dispersion of silicate layers in the polymer matrix up to 3 phr clay loading (Fig. 7a, b). Figure 7c exhibits the low-magnification morphology of $PUCB_5$ filled with 5 phr of organoclay loading. The image shows intercalation of silicate layers throughout the PU matrix instead of exfoliation. This is due to the fact, with the increase in clay content in the PU matrix, filler–filler interaction is predominant over the polymer–filler interaction. When compared with the modified one, the unmodified clay layers are totally agglomerated and aggregated at 3 wt% of loading both in high- and low-magnification TEM images (Fig. 6d and 7d). It is quite clear that, due to the presence of organic moiety in the modified silicates, the dispersion of silicates in polyurethane changes from an intercalated to an exfoliated structure. This kind of morphology in the nanocomposites is anticipated on account of the better compatibilization between the modified nanoclay and PU as already discussed in the earlier section. These results are in agreement with the XRD results, as shown earlier.

Dynamic mechanical thermal analysis

The DMTA can provide reliable information over the relaxation behavior of the materials examined. In order to evaluate the effect of the silicate layer nanoparticles into the PU matrix, thermomechanical properties have been measured. Due to the very high surface area of the nanoparticles in the PU nanocomposites and good dispersion, as observed in the earlier section, the applied stresses are expected to be easily transferred from the matrix onto the silicate layer, resulting in an enhancement of the mechanical properties. Finer dispersion of the nanoparticles could lead to a further enhancement of thermomechanical properties. The dynamic mechanical thermal data of the composites with different nature and loading of nanoclay are depicted in Fig. 8a, b, in the form of storage modulus (E') and loss tangent (tan δ), respectively. The results are given in Table 2. The storage modulus increases with the addition of clay. The moduli values above and below T_g are enhanced with increasing the clay content in the polymer matrix. For the nanocomposite with 5 wt% modified clay content ($PUCB_5$), the storage modulus is increased by about $\sim$300% at -40 °C and $\sim$295% at 25 °C as compared to the pure PU (PUP), indicating that incorporation of the nanoclay has reinforced the polymer matrix (Fig. 8a). These materials are often used

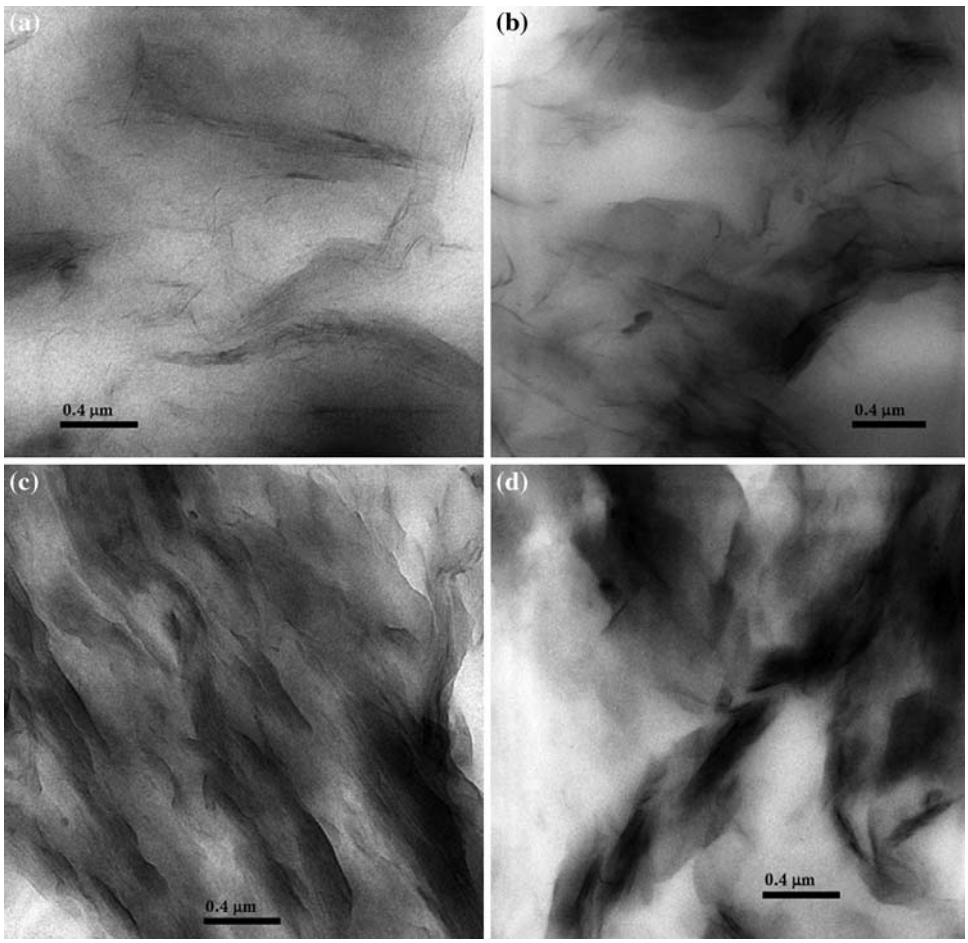

Fig. 7 Low-magnification TEM micrographs of different PUs at various clay loadings: **a** $PUCB_1$; **b** $PUCB_3$; **c** $PUCB_5$; **d** $PUNA_3$

at the temperature above their T_g, and hence, the changes in moduli above the T_g displays more practical significance than those below the T_g. In general, the enhancement in storage moduli (above T_g) for the polymer/clay nanocomposites is due to the reinforcement by clay particles together with the restricted segment mobility at the organic–inorganic interface neighborhood of the PU-modified clay nanocomposites for E' [25]. Chowdhury et al. [26] and Kader et al. [27] have reported the same trend for the carbon/epoxy–clay and nitrile rubber clay nanocomposites, respectively.

Usually the T_g of a polymer matrix tends to increase with the addition of nanoparticles, due the interactions between polymer chains and nanoparticles. In our case also, T_g is observed to increase in an approximately linear fashion with the increased addition of clay platelets (Fig. 8b). The results are in agreement with those reported by Maiti and Bhowmick [28] in the fluoroelastomer clay nanocomposites. For example, T_g for the neat PU (PUP) is −28 °C, whereas the same for the nanocomposite having 5 wt% loading of clay is −21 °C. An approximately 7 °C shift is observed with 5 wt% clay loading. The magnitude of the tan δ peak also decreases with an increase in the concentration of clay, shown in the same figure. Keya et al. [29] reported the same trend for the epoxy–clay nanocomposites. The tan δ peak for PUP observed at 0.25 reduces to 0.17 for $PUCB_5$. This is mainly attributed to good adhesion between the PU and the modified clay particles, as a result of which the nanometer-sized particles can restrict the segmental motion near the organic–inorganic interface.

The storage modulus of PU nanocomposites with 3 phr clay loading obtained from different modified (Cloisite 30B) and unmodified (Cloisite Na^+) clays can be compared. $PUCB_3$ nanocomposites prepared from the modified clays shows better dynamic mechanical property (Fig. 8). The value of storage modulus at 25 °C for $PUCB_3$ and $PUNA_3$ is 75 and 52 MPa, respectively. The tan δ peak position for $PUNA_3$ is almost the same as that of the pristine PU (PUP), indicating that there is an insignificant interaction with the polyurethane matrix. The modifier compound of Cloisite 30B with methyl, tallow, bis-2-hydroxyethyl, quaternary ammonium helps to interact with the polyurethane matrix. The difference in dynamic mechanical properties between the modified and the

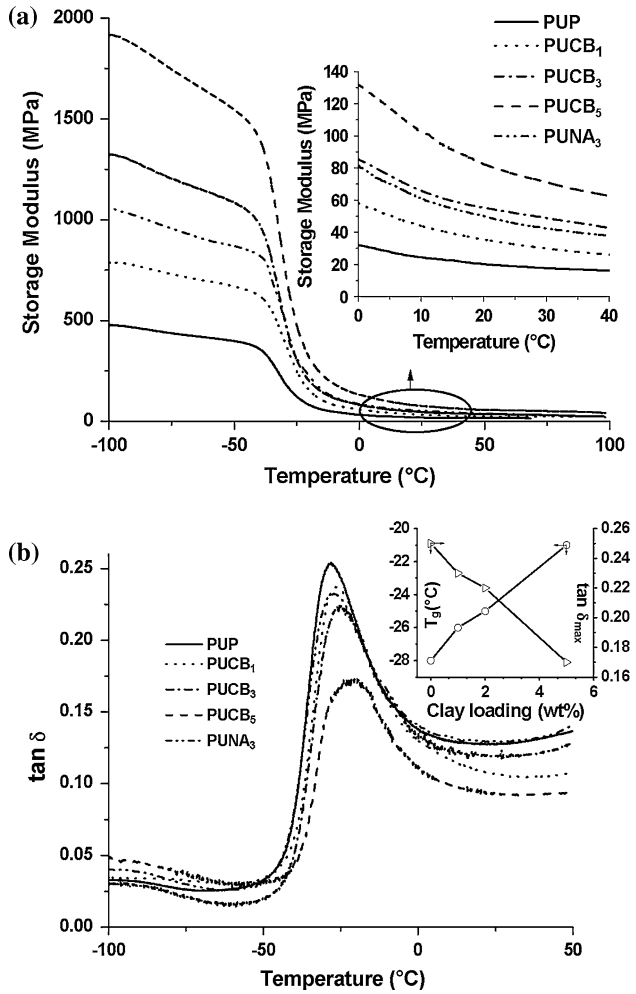

Fig. 8 **a** Storage modulus versus temperature, **b** tan δ versus temperature plots for different PU nanocomposites

unmodified clay-filled systems is considerably high, which indirectly proves that the dispersion of Cloisite Na^+ in PU matrix is poor. From the TEM micrograph (Fig. 6d and 7d), agglomeration of clay platelets is also observed in the case of PU nanocomposites containing 3 phr Cloisite Na^+ ($PUNA_3$).

Thermogravimetric analysis

Thermal stability of pristine PU and its nanocomposites from the unmodified and the modified clay at different loadings has been investigated by TGA. The degradation behavior of the nanocomposites is shown in Fig. 9a, b. The data obtained from these curves are given in Table 2, which shows the quantitative values of the onset degradation temperature (T_i), the temperature at which the maximum degradation takes place (T_{max}), and the rate of degradation for various PU nanocomposites. The thermal degradation of polyurethane occurs in two stages: the first stage is mainly governed by the degradation of the hard segment and the second stage correlates well with the degradation of the soft segment [30]. There is little effect of nanoclay on the hard segment degradation (all the samples show hard segment degradation temperature at ~304 °C). $PUCB_5$ shows the highest thermal stability and its T_i and T_{max} are about 26 and 23 °C, respectively, higher than those of the neat polyurethane. The rate of degradation is also lower than that of the pristine polyurethane, indicating higher thermal stability of the nanocomposites. In general, clay particles can enhance the thermal stability of the polymer by acting as the thermal insulator and mass transport barrier to the volatile products generated during decomposition.

The effect of nature of clay on the thermal stability is shown in Fig. 9a, b. Thermal insulator and mass transport barrier on thermal stability can be increased with improving the dispersibility of nanoclay; so T_{max} of $PUCB_3$ is about 5 °C higher than those of $PUNA_3$ due to good dispersibility of nanoclay (Figs. 6 and 7) in $PUCB_3$ nanocomposites. A similar result of thermal stability has also been reported for polypropylene/clay [31], polyethylene/clay [32], polystyrene/clay [33], and styrene-(ethylene-*co*-butylene)-styrene triblock copolymer/clay nanocomposites [34].

Tensile properties

The stress–strain behavior of all the nanocomposites reinforced with either the unmodified (Cloisite Na^+) or the

Table 2 Comparison of thermal properties of different polyurethane nanocomposites

Samples	DMA					TGA/DTG		
	T_g (°C)	E' at −40 °C (MPa)	E' at 0 °C (MPa)	E' at 25 °C (MPa)	tan δ_{max}	T_i (°C)	T_{max} (°C)	Rate of degradation (%/°C)
PUP	−28	355	31	19	0.25	354	393	1.89
$PUCB_1$	−26	628	59	32	0.23	362	398	1.79
$PUCB_3$	−25	1002	81	45	0.22	373	409	1.73
$PUCB_5$	−21	1438	131	75	0.17	380	416	1.67
$PUNA_3$	−27	832	86	52	0.23	368	404	1.77

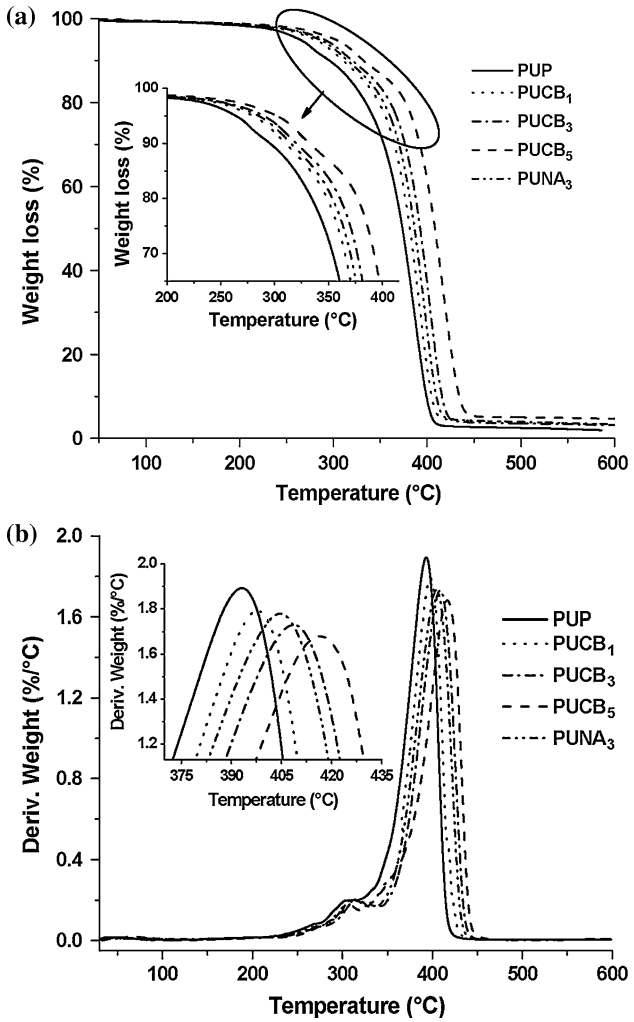

Fig. 9 **a** TGA and **b** DTG thermogram of PU nanocomposites

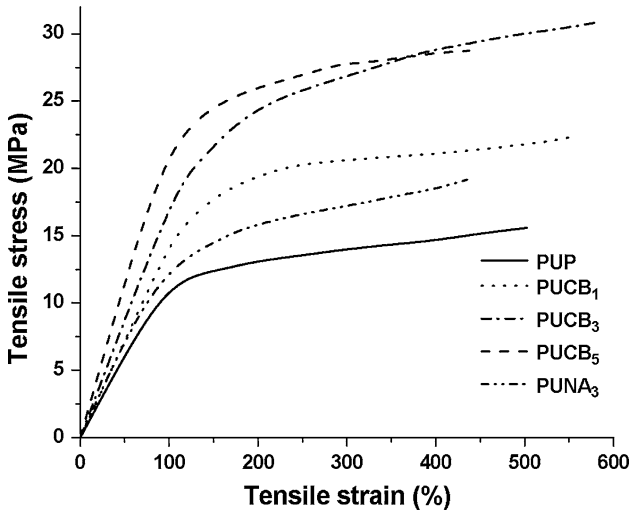

Fig. 10 Tensile properties of PU samples having different clay loadings

modified clay (Cloisite 30B) nanoparticles under tensile loading at room temperature is shown in Fig. 10. As the clay content increases, the strain to failure decreases at higher loading. The variation in tensile modulus as a function of clay content for these nanocomposites is given in Table 3. It is found that the modulus of the nanocomposites increases monotonically with increasing clay content. Both Cloisite Na^+/and Cloisite 30B/PU nanocomposites show a similar trend. However, at higher clay contents, the Cloisite 30B/PU nanocomposite displays a greater increase in modulus than the Cloisite Na^+/PU nanocomposite. There is a ~54 and ~17% increase of 100% modulus with the addition of 3 phr of the modified and the unmodified clay in PU matrix, respectively. The higher improvement of tensile modulus in Cloisite 30B/PU compared to Cloisite Na^+/PU can be attributed to the better dispersion and intercalation/exfoliation of the nanoparticles in the former case, as shown in Figs. 6 and 7b. In general, the improvement in tensile modulus is attributed to good dispersion of nano-sized clay particles and good interfacial adhesion between the particles and the PU matrix so that the mobility of polymer chains is restricted under loading. Highest increment in 100% tensile modulus is observed in $PUCB_5$.

With the increase in loading of clay, tensile strength increases up to 3 wt%, beyond which it decreases. $PUCB_3$ and $PUCB_5$ register tensile strength of 30.85 and 28.74 MPa, respectively. Above 3 wt% organoclay loading, the formation of a homogeneous nanostructure is more difficult. The organoclay layers are found in the form of agglomeration in the PU matrix, as shown in the XRD and TEM investigations. Due to the agglomeration of the nanofillers, the filler–filler interaction is predominant over the filler–polymer interaction. Also, agglomerated particles act as defects. Maiti et al. [35] reported the same trend of an increase in the tensile strength of ethylene–octene copolymer nanocomposites with clay loading. The addition of nanofillers has a synergistic effect on the tensile properties of the PUs. With the addition of nanoclays, even the elongation at break of the PU nanocomposites increases (by 11 and 16% for $PUCB_1$ and $PUCB_3$, respectively, over the pristine PU).

Adhesive properties

The effect of the nature and content of clay in the PU nanocomposites on the lap shear strength between aluminum and aluminum is shown in Fig. 11. Adhesive property of polyurethane nanocomposites has not been reported extensively. Incorporation of modified clay into the PU matrix results in an improvement of the joint strength up to a certain loading. 3 wt% addition of the modified clay in PU matrix shows 320% improvement over the pristine PU (PUP). Above 3 wt% modified clay loading, the dispersion

Table 3 Comparison of mechanical and adhesive properties of different polyurethane nanocomposites

Samples	Mechanical properties					Adhesive properties
	Tensile modulus (MPa) at % elongation			Tensile strength (MPa)	Elongation at break (%)	Lap shear strength (kN/m^2)
	100	200	300			
PUP	10.80 ± 0.23	13.09 ± 0.28	13.96 ± 0.32	15.57 ± 0.36	502 ± 10	1.9 ± 0.2
$PUCB_1$	13.96 ± 0.22	19.63 ± 0.27	20.61 ± 0.35	22.40 ± 0.36	559 ± 12	4.5 ± 0.3
$PUCB_3$	16.68 ± 0.21	24.53 ± 0.26	27.04 ± 0.34	30.85 ± 0.39	581 ± 13	8.0 ± 0.2
$PUCB_5$	20.83 ± 0.22	26.06 ± 0.31	27.91 ± 0.36	28.74 ± 0.40	438 ± 17	5.0 ± 0.1
$PUNA_3$	12.32 ± 0.25	15.92 ± 0.32	17.23 ± 0.36	19.16 ± 0.41	435 ± 19	4.3 ± 0.2

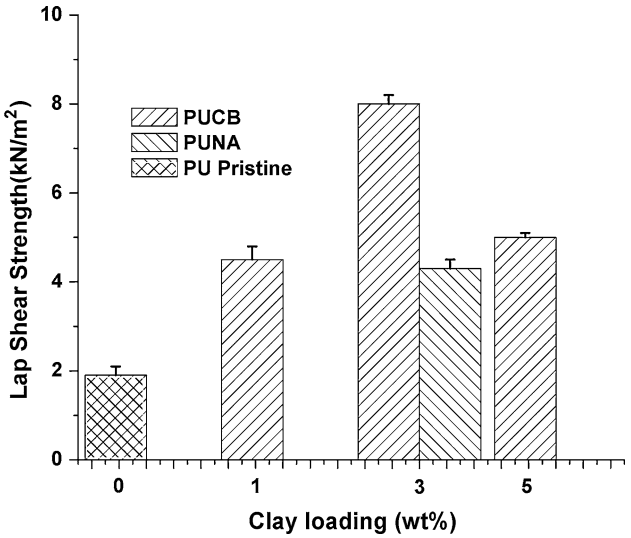

Fig. 11 Lap shear strength between aluminum and aluminum with PU adhesive having different clay loadings

is more difficult. Unmodified clay has a little effect on the adhesive properties of PU matrix. Patel et al. [36] reported the same trend of an increase in adhesive strength with the addition of nanoclay in an acrylic adhesive. The lap shear strength values are 4.3 and 8.0 kN/m^2 for 3 wt% unmodified clay and modified clay-filled systems, respectively. It is also evident from the XRD and TEM that it is difficult to disperse the unmodified clay in the PU matrix. The superior reinforcement of the polymer matrix by the modified clay platelets probably plays a key role in increasing the cohesive strength of the base polymer and thus increases the joint strength. The failure patterns in the lap joints are of cohesive type. These confirm the existence of the strong interfacial reactions at the adhesive/substrate interface. The OH groups (from the modifier compound of Cloisite 30B) on the clay surface may form strong interfacial hydrogen bonds with the Al–OH groups on the aluminum surface. This will enhance the clay/metal adhesion. Since the clay platelets are dispersed well in the polymer matrix, it seems that the nanoclay particles can act as an interphase between the aluminum adherent and the polymer, and thereby help in better adhesion. In line with this, the lap strength increases with the increase in the clay concentration.

Moreover, it is clear from the tensile properties that the addition of nanoclay has significantly increased the elongation at break values of the PU-modified clay nanocomposites along with the high increment in the tensile strength values. This suggests the good ductile nature of the PU nanocomposites as well as higher strain energy density in comparison with the unfilled PU adhesive (PUP). The ductile materials can dissipate greater amount of energy during the bond rupture process in the lap shear test, which will result in good joint strength. Therefore, it seems that the addition of nanoclay to PU adhesive will result in nanocomposite adhesive with good strength and ductility.

Conclusions

Polyester polyurethane nanocomposites incorporating modified and unmodified nanoclays have been prepared. The nanocomposites derived from the modified clay provide the best mechanical, dynamic mechanical, thermal, and adhesive properties. For examples, there are ~100, ~135, and ~300% improvement in tensile strength, storage modulus at 25 °C, and lap shear strength, respectively, at 3 phr of the modified clay loading. This is because of the favorable interaction between the PU matrix and the modified clay due to the presence of organic moiety in the modified silicates. The excellent degree of dispersion of the modified clay in the nanocomposites as evaluated by TEM and XRD is also responsible. At higher contents (above 3 phr), agglomeration of the clays causes non-uniform dispersion, resulting in lowering of the mechanical and adhesive properties.

Acknowledgement The financial support of this study by Indian Space Research Organization (ISRO), India, is gratefully acknowledged.

References

1. Ray SS, Okamoto M (2003) Prog Polym Sci 28:1539
2. Giannelis EP (1996) Adv Mater 8:29
3. Ke YC, Stroeve P (2005) Polymer-layered silicate and silica nanocomposites. Elsevier, Amsterdam, The Netherlands
4. Bhowmick AK (ed) (2008) Current topics of elastomers research. Taylor & Francis Inc., CRC Press, USA
5. Sridhar LN, Gupta RK, Bhardwaj M (2006) Ind Eng Chem Res 45:8282
6. Bose NK, Kamal MR (2009) Polym Eng Sci 49:641
7. Lee CH, Kim HB, Lim ST, Choi HJ, Jhon MS (2005) J Mater Sci 40:3981. doi:10.1007/s10853-005-2818-6
8. Maiti M, Bhattacharya M, Bhowmick AK (2008) Rubber Chem Technol 81:384
9. Bhattacharya M, Bhowmick AK (2008) Polymer 49:4808
10. Sadhu S, Bhowmick AK (2005) Rubber Chem Technol 78:321
11. Chung SK, Wie JJ, Park BY, Kim SC (2009) J Macromol Sci A Pure Appl Chem 46:205
12. Ganguly A, Bhowmick AK (2008) Nanoscale Res Lett 3:36
13. Maiti M, Bhowmick AK (2009) J Appl Polym Sci 111:1094
14. Schollenberger SC (2001) In: Bhowmick AK, Stephens HL (eds) Handbook of elastomers, 2nd edn. Marcel Dekker Inc., USA
15. Wang Z, Pinnavaia T (1998) J Chem Mater 10:3769
16. Zilg C, Thomann R, Mulhaupt R, Finter J (1999) Adv Mater 11:49
17. Xu R, Manias E, Snyder AJ, Runt J (2001) Macromolecules 34:337
18. Maji PK, Guchhait PK, Bhowmick AK (2009) ACS Appl Mater Interface 1:289
19. Sadhu S, Bhowmick AK (2005) J Mater Sci 40:1633. doi:10.1007/s10853-005-0663-2
20. Sengupta R, Ganguly A, Sabharwal S, Chaki TK, Bhowmick AK (2007) J Mater Sci 42:923. doi:10.1007/s10853-006-0011-1
21. Hepburn C (1982) Polyurethane elastomers. Applied Science Publishers Ltd., England
22. David DJ, Staley HB (1969) Analytical chemistry of the polyurethane. Wiley Interscience, USA
23. Kim KJ, Lee JS, Prabu AA, Kim TH (2009) Polym Compos 30:265
24. Zhang J, Wilkie CA (2006) Polymer 47:5736
25. Xiong J, Zheng Z, Jiang H, Ye S, Wang S (2007) Composites A Appl Sci Manuf 38:132
26. Chowdhury FH, Hosur MV, Jeelani S (2007) J Mater Sci 42:2690. doi:10.1007/s10853-006-1370-3
27. Kader MA, Kim K, Lee YS, Nah C (2006) J Mater Sci 41:7341. doi:10.1007/s10853-006-0792-2
28. Maiti M, Bhowmick AK (2007) Polym Eng Sci 47:1777
29. Keya E, Tanoglu M, Okur S (2008) J Appl Polym Sci 109:834
30. Petrovic ZS, Zavargo Z, Flynn JH, Macknight WJ (1994) J Appl Polym Sci 51:1087
31. Kodgire P, Kalgaonkar R, Hambir S, Bulakh N, Jog JP (2001) J Appl Polym Sci 81:1786
32. Lu H, Hu Y, Yang L, Wang Z, Chen Z, Fan W (2005) J Mater Sci 40:43. doi:10.1007/s10853-005-5685-2
33. Fu X, Qutubuddin S (2001) Polymer 42:807
34. Ganguli A, Bhowmick AK (2009) J Mater Sci 44:903. doi:10.1007/s10853-008-3183-z
35. Maiti M, Sadhu S, Bhowmick AK (2006) J Appl Polym Sci 101:603
36. Patel S, Bandyopadhyay A, Ganguly A, Bhowmick AK (2006) J Adhes Sci Technol 20:371